NASA TECHNICAL TRANSLATION NASA TT F-11,694

NASA TT F-11,694

CHARACTERISTICS METHOD FOR COMPUTING TWO-DIMENSIONAL EQUILIBRIUM AND PERFECT GAS VORTEX FLOWS

Yu. N. D'yakonov, L. V. Pchelkina and I. D. Sandomirskaya

Translation of "Metod Kharakteristik dlya Rascheta Dvumernykh Vikhrevykh Techeniy Ravnovesnogo i Sovershennogo Gaza"
In: Vycheslitel'nyye Metody i Programmirovaniye. Chislennyye Metody v Gazovoy Dinamike
Sbornik Rabot Vychislitel'nogo Tsentra MGU, No. 7, Moscow University Press, pp. 206-224, 1967

NATIONAL AERONAUTICS AND SPACE ADMINISTRATION
WASHINGTON, D. C. 20546 MAY 1968

NASA TT F-11,694

CHARACTERISTICS METHOD FOR COMPUTING TWO-DIMENSIONAL EQUILIBRIUM AND PERFECT GAS VORTEX FLOWS

Yu. N. D'yakonov, L. V. Pchelkina and I. D. Sandomirskaya

ABSTRACT. After briefly discussing the merits of the nets and characteristics methods for computing supersonic flow regions, the authors propose and describe a possible scheme for using the characteristics method for computing a steady, two-dimensional vortex flow of a perfect gas, and particularly of an equilibrium gas flow at $M_\infty = 6$ past blunt bodies. The scheme is so designed as to be suitable for computerized solution with or without taking equilibrium physical-chemical reactions into consideration. The results of several computerized solutions are presented graphically. Analysis of results reveals quantitative and qualitative differences in gas flow patterns in vortex layers for plane and axisymmetric flows past blunted bodies.

Aircraft designed for operation at high supersonic speeds generally have blunted aerodynamic form. As a supersonic gas stream flows around a body with blunted bow, a receding shock wave develops in front of the body, and the flow in the shock layer is mixed in nature (Figure 1): near the bow portion, there is an area of subsonic velocities ABCD, closed by sonic line CD; further, an area of supersonic flow arises. Limiting characteristic DE (or two limiting characteristics of different sets) sets off the minimum area of influence. Calculation of this type of flow generally includes two stages: calculation of the subsonic and transonic area, and calculation of the purely supersonic area, which is performed using the initial data produced as a result of solution of the first stage of the problem. /206[1]

In calculating the supersonic flow area with zero and nonzero angles of attack, the most widely used methods in recent times have been the nets method [1-5] and a method based on the idea of characteristics [6-12]. It should be noted that some methods (particularly the methods of [8, 9, 11]) using characteristics relationships in some form, essentially occupy an intermediate [illegible] and the characteristics method itself.

In many cases, the nets method has certain advantages over the characteristics method: with an identical number of calculation points, it is more economical (particularly in solving three-dimensional problems), and is simple in its logic; the results produced are convenient for analysis of the flow field of the gas in the shock layer, since they are presented in layers with predetermined geometry; where necessary, depending on the nature of the change in

[1] Numbers in the margin indicate pagination in the foreign text.

the parameters, the step of the net can be reduced with respect to certain variables or, on the other hand, increased in some portion of the shock layer, etc. /207

Still, it should be considered that the flow about a blunt body has a complex, nonanalytic nature with large gradients of the gas parameters. The characteristic HL (see Figure 1) beginning at the point of contact between the blunted tip and the straight line sector of the contour, divides the supersonic area into two parts: the area located to the right of this characteristic is an area of influence of the straight line surface, while area CDHL is the portion of the supersonic flow area influenced by the blunt tip. Since two essentially different solutions are "stuck together" along characteristic HL, the first derivatives of the flow parameters are discontinuous across the characteristic, and the gas dynamic functions are represented by broken curves. As this characteristic is reflected from the head wave, two other lines of weak discontinuity appear: the reflected characteristic LM, and the flow line LN. Characteristic LM is in turn reflected from the wall, etc.

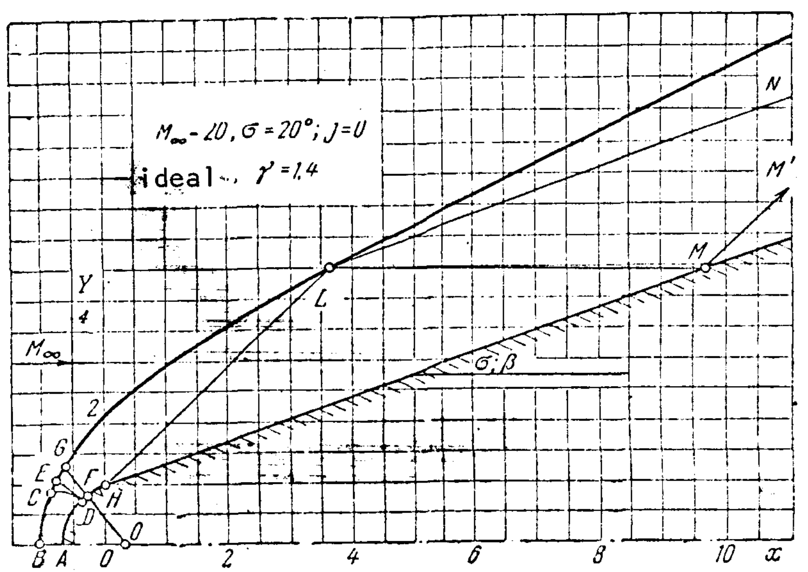

Figure 1. Picture of Flow During Supersonic Flow About a Blunted Body

Also, singularities may occur in the shock layer, related to the presence of a thin vortex layer near the surface of the body, the formation of limit lines, hanging shock waves, etc. /208

Investigation of this type of singularity is more naturally and conveniently performed using the characteristics method.

In this work, we analyze one possible scheme for using the characteristics method for the calculation of stable, two-dimensional vortex flows. Since the results from calculations of the flow about blunted bodies by ideal gases, particularly equilibrium gases (at Mach numbers $M_\infty \geqslant 6$) are of considerable interest, the characteristics method scheme was selected such that the corresponging digital computer program is universal, i.e. can be used to calculate flows either with or without consideration of equilibrium physical and chemical reactions. Certain results of the calculations of flow about blunted flat and axisymmetrical bodies by a supersonic flow of an ideal ($\gamma = 1.4$) and equilibrium gas (air) are presented. Some of the data presented were produced using the nets method, as used in [4]. An analysis is presented of the results of calculation, and they are compared with certain conclusions from the theory of hypersonic flows.

§1. Calculation Method

Let us write a system of gas dynamics equations for a stable flow of an inviscid and non-heat conducting gas considering the equilibrium physical-chemical reactions in the following form [4]:

$$\rho(\overline{w}, \nabla) w = - \operatorname{grad} p,$$

$$(\overline{w}, \operatorname{grad} \ln p) = (\overline{w}, \varkappa \operatorname{grad} \ln \rho),$$

$$\operatorname{div}(\rho \overline{w}) = 0,$$

$$\varkappa(p, \rho) = \left(\frac{d \ln p}{d \ln \rho}\right)_s = \frac{\rho a^2}{p} \Bigg| \quad \text{is a known function.}$$

In the particular case $\kappa = \gamma = \text{const}$, we produce a system of equations corresponding to the flow of an ideal gas.

In order to approximate the effective isentropy index κ and other equilibrium thermodynamic functions, let us use a method suggested in [4].

The differential equations of the characteristics and relationships based on them can be represented in the following form:

$$d\theta \pm \frac{\sin\mu \cos\mu}{\varkappa p} dp \pm j \frac{\sin\theta \sin\mu}{y \sin(\theta \pm \mu)} dy = 0,$$

$$\frac{dy}{dx} = \operatorname{tg}(\theta \pm \mu)$$

along the characteristics of the first and second sets; and /209

$$\frac{dy}{dx} = \operatorname{tg}\theta,$$

$$w\,dw + \frac{dp}{\rho} = 0,$$

$$a^2 = \frac{dp}{d\rho} = \varkappa\frac{p}{\rho}$$

along the flow lines;

$\kappa = \kappa(p,\rho)$ is a known function;

where j = 0 for a two-dimensional flow and j = 1 for an axisymmetrical flow. In the above relationships, we have used the usual symbols: x,y are cylindrical or Cartesian coordinates; μ = arcsin 1/M is the Mach angle; w is the modulus of the velocity vector; θ is the inclination angle of the velocity vector to the x axis.

Let us introduce the new desired functions

$$\zeta = \operatorname{ctg}\mu,\ \delta_* = \operatorname{tg}\frac{\theta}{4},$$

similar to those suggested by Ehlers [12].

In order that the characteristics method might allow us to use a single program to calculate flows with or without consideration of equilibrium physical and chemical reactions, let us select the following functions as those to be sought: x, y, δ_*, p, ρ, w. Now, in consideration of (3), the main system of equations (2) can be written in the form

$$\frac{4d\delta_*}{1+\delta_*^2} \pm \frac{\zeta dp}{\rho w^2} \pm j\frac{A\,dx}{y(\zeta B \mp A)} = 0;$$

$$\frac{dy}{dx} = \frac{\zeta A \pm B}{\zeta B \mp B}$$

along the characteristics of the first and second sets; and

$$\frac{dy}{dx} = \frac{A}{B}; \quad w\,dw + \frac{dp}{\zeta} = 0; \quad a^2 = \frac{dp}{d\rho} = \varkappa \frac{p}{\rho}$$

along the flow line;

$\kappa = \kappa(p,\rho)$ is a known function,

where

$$A = \delta_*(1 - \delta_*^2), \quad B = \left(\frac{1 - \delta_*^2}{2}\right)^2 - \delta_*^2.$$

The boundary conditions of the problem are: at the surface of the body fixed by equation $y = \Phi(x)$, the condition of zero flow through the surface

$$v - u\Phi_x = 0,$$

and at the shock wave, the primary laws of conservation /210

$$\left.\begin{aligned} p_\infty + \rho_\infty w_{n\infty}^2 &= p_w + \rho_w w_{nw}^2; \\ \rho_\infty w_{n\infty} &= \rho_w w_{nw}; \\ h_\infty + \frac{w_{n\infty}^2}{2} &= h_w + \frac{w_{nw}^2}{2}, \\ u_\infty - u_w + F_x(v_\infty - v_w) &= 0. \end{aligned}\right|$$

where the subscript ∞ relates to the parameters of the unperturbed flow, the subscript w to the parameters immediately beyond the shock wave; the subscript x represents differentiation with respect to x; $y = F(x)$ is the equation for the surface of the shock wave; u, v are projections of velocity vector $\bar{w}$ on the x and y axes respectively; w_n is the component of the velocity vector perpendicular to the shock wave surface:

$$w_n = \frac{\bar{w}\,\mathrm{grad}\,F}{|\mathrm{grad}\,F|}.$$

In the case of flows of an equilibrium gas, we must add the following dependence to formulas (6):

$$h = h(p, \rho). \tag{7}$$

In performing our calculations, in place of the third relationship of (6), we use the following dependence, calculated in advance for a direct compression jump:

$$\frac{p_w}{p_\infty} = f(M_\infty, p_\infty, T_\infty), \tag{8}$$

which was approximated by sectors using second power polynomials with an accuracy of 0.1-0.5%.

As is shown in [4], dependence (7) can be quite simply and economically approximated throughout the entire range of pressures and temperatures of tables [13-15]. Then, the equations on the shock wave can be solved using system (6)-(7). This eliminates the necessity of fixing dependence (8) in advance, and makes it possible to calculate flows in which equilibrium physical and chemical conversions of the gas have an essential role to play in the oncoming stream.

As we know, the characteristics method includes the solution of the following basic problems: calculation of an internal point in the field, located at the intersection of the two characteristics of the different sets; calculation of a point lying on the surface of the body; calculation of a point on the shock wave. In order to calculate the values of quantities x, y, δ_*, p, ρ and w at some point "c" on the basis of their known values at points "a" and "b," the corresponding differential equations of system (4) are represented in finite-difference form. The system of equations produced is solved by the iterations method, all the coefficients in the first iteration being determined from values of the functions at points "a" and "b" respectively; in subsequent approximations, the mean values of the coefficients for points "a" and "c" or "b" and "c" are taken. In order to produce good accuracy, it is usually sufficient to make three approximations. Determination of the parameters at the point of intersection of the flow lines originating at point "c" with the line on which all gas parameters have already been calculated (calculated characteristic or line of initial data) is performed using quadratic interpolation with respect to the corresponding nodal points lying on this line. /211

All calculations were performed along the characteristics of the second set. In the process of calculations, strong variations in the locations of the nodal points on the characteristic can occur. In connection with this, equilibration of points was performed periodically using quadratic interpolation. Equilibration was generally performed on reflected characteristics of the second set, corresponding to various discontinuous characteristics of the first set (for example, characteristic LM -- see Figure 1).

The value of κ was calculated by quadratic interpolation with respect to values $\kappa_k = \kappa_k(\ln p_i, q_j)$ determined from the table, where q is a certain function of pressure and density (see [4]). The accuracy of the approximation of κ is on the order of 1%. Here, in order to approximate the effective isentropy index throughout the entire range of parameters, approximately 300 digital computer memory locations were used in [13-15].

Times required for calculation of the flow around a blunt body by equilibrium and ideal gases are practically identical.

The initial data on ray OG (see Figure 1) both in the case of equilibrium air and in the case of an ideal gas were calculated by the method suggested by G. F. Telenin [16-18].

The velocities were related to the value of the critical speed of sound a_*, calculated for an ideal gas with constant adiabatic index $\gamma = 1.4$; the density was related to the density of the oncoming flow; pressure was related to the quantity $\rho_\infty a_*^2$. In calculating flow around blunt bodies both by ideal and by equilibrium gases, all parameters were related to these quantities.

All checks of the solution (similar to those performed in [3-5]) as well as comparisons with the results of calculations by the nets method [3-5] showed that the accuracy of the data produced is on the order of 1%.

§2. Results of Calculations, Some Specific Features of the Flow of Equilibrium and Ideal Gases Around Flat and Axisymmetrical Blunt Bodies /212

In correspondence with the characteristics method outlined, a program was composed for a digital computer and calculations of the flow around two-dimensional (j = 0) and axisymmetrical (j = 1) bodies were calculated using various forms of blunting of the front portion of the body, for a supersonic flow of an ideal ($\gamma = 1.4$) or equilibrium gas (air).

The number of nodal points on the characteristics in the second set was varied from n = 40 to n = 200, depending on the nature of the flow being studied.

The calculations of the flow of an ideal gas around wedges blunted in the form of a circle were performed in the range of Mach numbers $M_\infty = 4$-20 with half apex angle $\sigma = -20°$-$+20°$.

The flow around blunted cones by a stream of an ideal and equilibrium gas was investigated in the range of Mach numbers $M_\infty = 6$-∞, of half apex angles $\beta = -30°$-$+20°$, of pressures in the oncoming stream $p_\infty = 0.0001$-1.0 bar, of temperatures $T_\infty = 200$-$300°K$. The blunting studied had the form of ellipsoids of rotation, the ratio of the vertical and horizontal axes varying within limits $1/3 \leqslant \delta \leqslant 3$.

Let us analyze some specific features of the flow of the gas around the two-dimensional and axisymmetrical blunt bodies using the results of calculation shown on Figures 1-12.

First of all, let us note the relative increase in thickness of the shock layer in the case of two-dimensional flow over the corresponding axisymmetrical gas flow (cf. Figure 1 and the data of [4]).

The distribution of pressure on the surface of the wedge and on the shock wave is shown on Figure 2. The value x = 0 corresponds to the point of contact of the cylinder with the wedge, and readings on the x axis are given in units of the blunting radius. The x axis is always directed parallel to the velocity vector of the oncoming stream.

As we can see from the data on Figure 2, in the area of the point of contact, in the downstream direction, a considerable positive pressure gradient develops. In connection with this, the characteristics of the first set, having their origin at the wall in the area of the point of contact, have a tendency to converge. Since the shock layer is rather thick in the case of flow around two-dimensional bodies, before the discontinuous characteristic HL (Figure 1) reaches the surface of the head shock wave, the characteristics of the first set may begin intersecting, leading to the appearance of a limit line and the formation of a hanging shock wave in the flow. This type of singularity was observed in calculating flow around a wedge with a cylindrical blunted tip and /213 various angles σ at $M_\infty = 4$.

With larger M_∞ numbers, the shock layer becomes considerably thinner; therefore, generally speaking, the intersection of characteristics may not occur. In particular, where $M_\infty = 20$, $\sigma = 20°$, this singularity was not observed, in contrast to the situation which obtained at $M_\infty = 4$ (see Figure 2).

The data on Figures 1 and 2 also clearly illustrate the propagation of the weak perturbation (discontinuity of first derivatives of gas parameter resulting from discontinuity in curvature of contour at point H where cylinder contacts wedge) from the surface of the body into the flow, and its reflection from the head shock wave and from the wall. At point L, the discontinuous characteristic reaches the shock wave and results in the appearance of a considerable positive pressure gradient downstream from this point. The reflected characteristic of the second set arrives at the body surface at point M; when it is reflected from the shock wave, in correspondence with the conclusions of the theory of hypersonic flows [19], the perturbation changes its sign and becomes considerably weaker. Point M' on Figures 1 and 2 corresponds to the point of arrival of the next discontinuous characteristics of the first set at the surface of the head shock wave. This characteristic MM' is in turn reflected from the shock wave, etc.

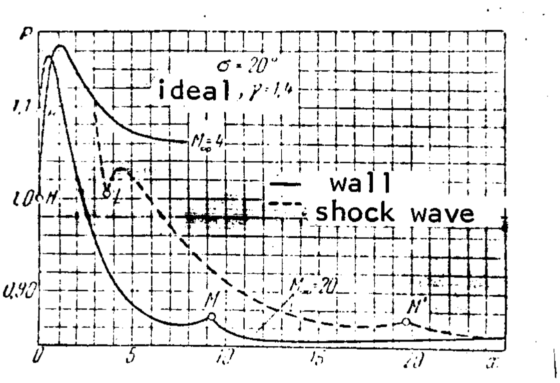

Figure 2. Distribution of Pressure on Surface of Body and on Shock Wave with Flow Around a Blunt Wedge

Figures 3-6 show the results of comparison of the fields of gas parameters p, δ_*, ρ and the M number along the characteristics of the second set in the case of two-dimensional and axisymmetrical flow. The coordinate $\xi = (x - x_s)/(x_w - x_s)$, where the subscripts s and w mean that the point belongs to the surface of the body or to the shock wave. Figure 3 also shows the values of x_s corresponding to the three /214
characteristics 1, 2 and 3 of the two-dimensional flow and three characteristics 1', 2' and 3' of the axisymmetrical gas flow.

In the case of a two-dimensional flow, the data on Figures 3-6 clearly illustrate the nature of the change in gas parameters in each of the areas shown on Figure 1 and separated from each other by the weak discontinuity surfaces: the discontinuous characteristic of the first set HL, flow line LN, reflected discontinuous characteristic MM'. With axisymmetrical flow, the corresponding discontinuities are considerably weaker and the picture of the field of parameters is not as clear as with two-dimensional gas flow.

Analysis of the results produced allows us to determine not only the quantitative, but also the qualitative differences in the nature of the movement of the gas in the vortex layer in the case of flow around two-dimensional and axisymmetrical blunt bodies. This difference is as follows.

With axisymmetrical flow, since the flow rate of the high entropy gas passing through the strong shock wave near the tip of the body is finite, due to outward flow along the side surface of the cone, a thin layer is formed near the wall (usually called the vortex or entropy layer) with high transverse gradients of pressure and velocity. The formation of this layer can be easily seen on /215
Figures 5 and 6. It is interesting that throughout almost the entire shock layer, the flow lines are directed toward the body (Figure 4), i.e. as the length of the blunted cone increases, the vortex layer becomes ever thinner.

A different picture is observed with flow around a blunted wedge. In the initial sector of the shock layer, the flow lines are even directed away from the body (Figure 4); thus, the gas particles which have passed through the strong shock wave tend to occupy a relatively greater portion of the shock layer, and only with rather high values of x do the directions of the velocity vectors become almost constant, parallel to the generatrix of the wedge. This means that in the physical coordinates x and y, the thickness of the vortex layer of gas does not decrease although, if we use the relative coordinate ξ introduced above, with increasing x this layer will occupy a smaller fraction of the shock layer with respect to ξ, since the absolute size of the shock layer increases.

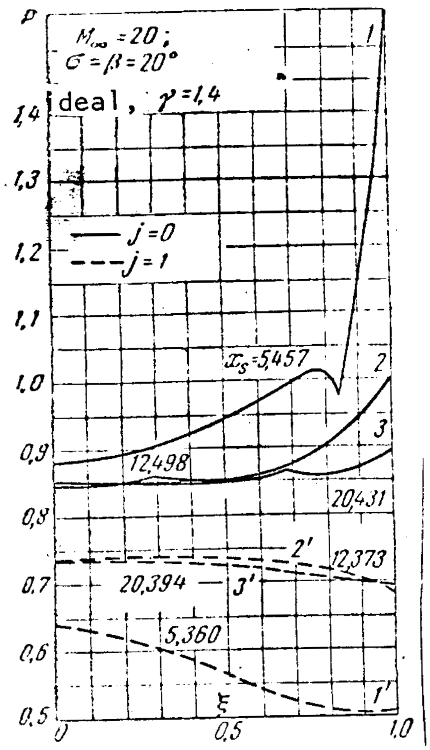

Figure 3. Distribution of Pressure Along Characteristics of Second Set

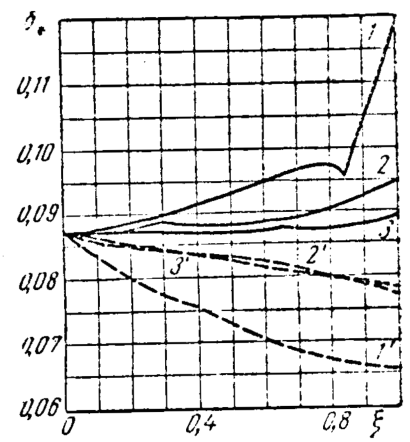

Figure 4. Distribution of δ_8 Along Characteristics of Second Set (symbols as on Figure 3)

Consequently, with flow around a blunted wedge, the vortex layer, in the sense in which it is usually used for axisymmetrical bodies, is absent, and in its place at large values of wedge length we find a gas layer of approximately /217
constant thickness (in physical coordinates x,y), which has passed through the strong shock wave near the bow portion of the body (for example, the gas layer arriving at the shock wave from the plane of symmetry y = 0 to point L or M' -- see Figures 1 and 2).

The data on Figures 5 and 6 also show that actually the computational difficulties noted in [3-5] related to the nature of the gas flow in the entropy layer are of the same order of magnitude both for the nets method and for the characteristics method.

In the case of flow around a blunted body by an ideal gas, any gas dynamics parameter in the shock layer depends, generally speaking, on coordinates x,y, the form of the blunting, the characteristic angle of inclination of generatrix

β, the M_∞ number and the ratio of specific heat capacities γ. If equilibrium physical-chemical reactions are taken into consideration, the pressure and temperature in the oncoming stream must be added to the number of primary determining parameters, as well as a parameter considering the thermodynamic properties of the gas being examined (an analog of the adiabatic index γ).

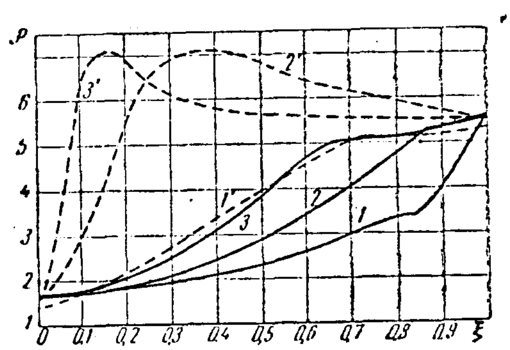

Figure 5. Distribution of Density Along Characteristics of Second Set (symbols as on Figure 3)

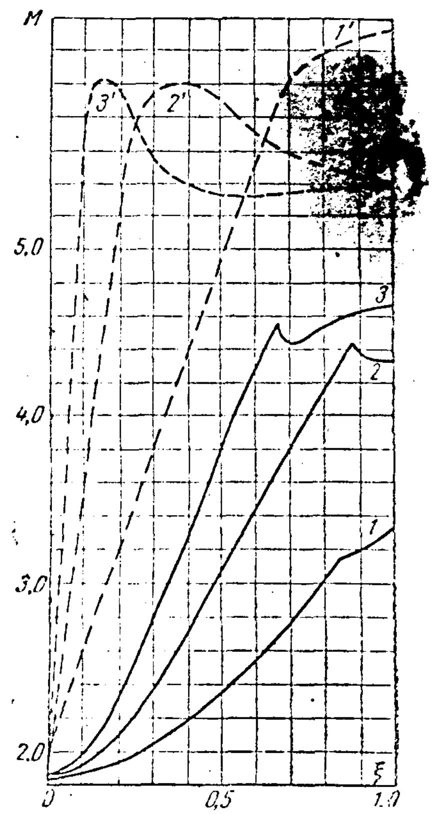

Figure 6. Distribution of M Numbers Along Characteristics of Second Set (symbols as on Figure 3)

Using the concepts concerning a strong explosion and an unstable analog to the methods of the theory of hypersonic flows, certain asymptotic relationships have been produced -- the so-called similarity laws [19], which are quite useful for the analysis and processing of experimental and calculated data. The similarity law states that for affine-similar bodies (regardless of the form of the blunting of the bow) the values of relative pressure on the body surface $P = (p_s - p_\infty/\rho_\infty w_\infty^2 \tau^2)$, relative inclination of the head wave to the direction of the oncoming stream $\xi = \tan \omega/\tau$ and relative drag coefficient $\bar{C}^*_x = C_x/\tau^*$ /219
depend, in the case of an ideal gas, on three dimensionless parameters: $k = M_\infty \tau$, $\eta = \sqrt{2/C_{x_0}} \cdot (x/d)\tau^2$ and γ. The quantity w_∞ represents the velocity vector

modulus of the unperturbed flow, τ and τ [sic -- Tr.] are the relative thicknesses of the body, ω is the angle of inclination of the shock wave to the x axis, C_{x0} is the drag coefficient of the blunt portion, and d is the diameter of the blunt portion. In particular, where $M_\infty = \infty$ for blunt cones, the values of P, ζ and $\bar{C}_x$ will depend only on two parameters: η and γ. As relative thicknesses of the body, we select the values $\tau = \tan\beta$ and $\tau_* = \sin\beta$.

Figures 7-12 show some results of investigations in variables of similarity for the flow around blunt cones by a stream of an equilibrium and ideal gas. Two characteristic variants were selected as the primary variants: in the case of the ideal gas, $\delta = 1$, $\beta = 10°$, $M_\infty = \infty$ (or 20), $\gamma = 1.4$; in the case of equilibrium air, $\delta = 1$, $\beta = 10°$, $M_\infty = 20$, $p_\infty = 0.01$ bar, $T_\infty = 250°K$. In performing calculations, all parameters in these variants were fixed with the exception of one parameter (taken in turn) which was varied over the range of change indicated above.

Analysis of the data on Figures 7-12 shows that in similarity variables, the curves converge strongly, although the differences do remain noticeable. In particular, the results produced are quite hopeful in the sense of the usage of this type of processing of data to determine the distribution of gas parameters with good accuracy with other forms of bow blunting on the basis of the results produced without performing additional calculation (curves 5, 7, 8 on Figures 9-12). The correspondence of these curves with various angles β and numbers M_∞ with fixed values of the remaining parameters is also satisfactory, but not as good as occurred in the investigation of the influence of the form of blunting. It should be noted that when the investigations were performed, the condition of similarity was not maintained in many variants for all of the dimensionless determining parameters included in the law of similarity, in particular for the parameter $k = M_\infty \tan\beta$, which becomes important where $M_\infty < \infty$. /220 /221

Thus, the similarity variables in the case of the flow of both an ideal and an equilibrium gas can be successfully used to produce various gas dynamic quantities with sufficient accuracy using data already available. Nevertheless, in order to provide high accuracy over a broad range of parameters, it is still necessary to accumulate rather voluminous numerical material.

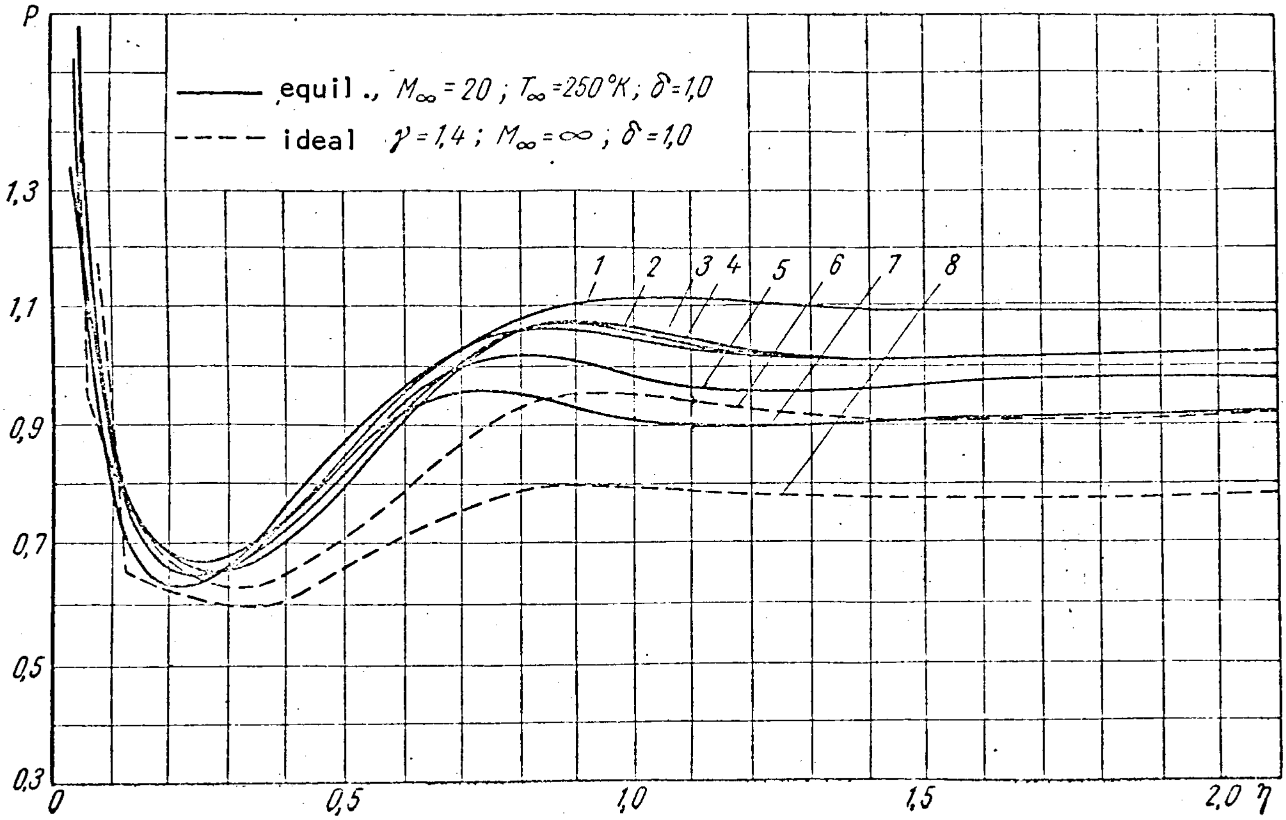

β	$C x_0$	p_∞ [бар]
1—5°	0,908	0,01
2—10°	0,923	1,00
3—10°	0,926	0,01
4—10°	0,930	0,0001
5—15°	0,956	0,01
7—20°	0,997	0,01
6—20°	0,974	
8—30°	1,086	

Figure 7. Pressure on Surface of Blunted Cone in Similarity Variables for the Case of Flow of an Ideal and Equilibrium Gas (Air)

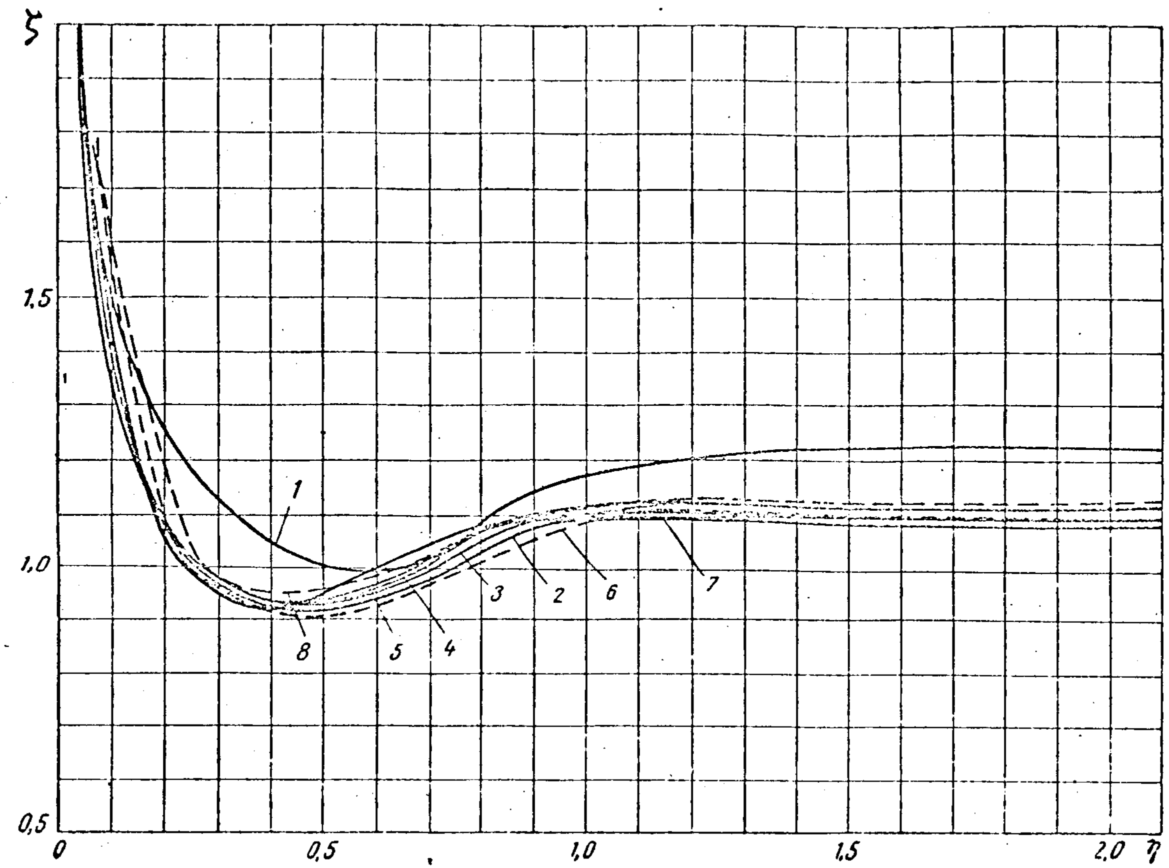

Figure 8. Inclination of Head Wave to Direction of Oncoming Stream in Similarity Variables for Flow Around Blunted Cone (symbols as on Figure 7)

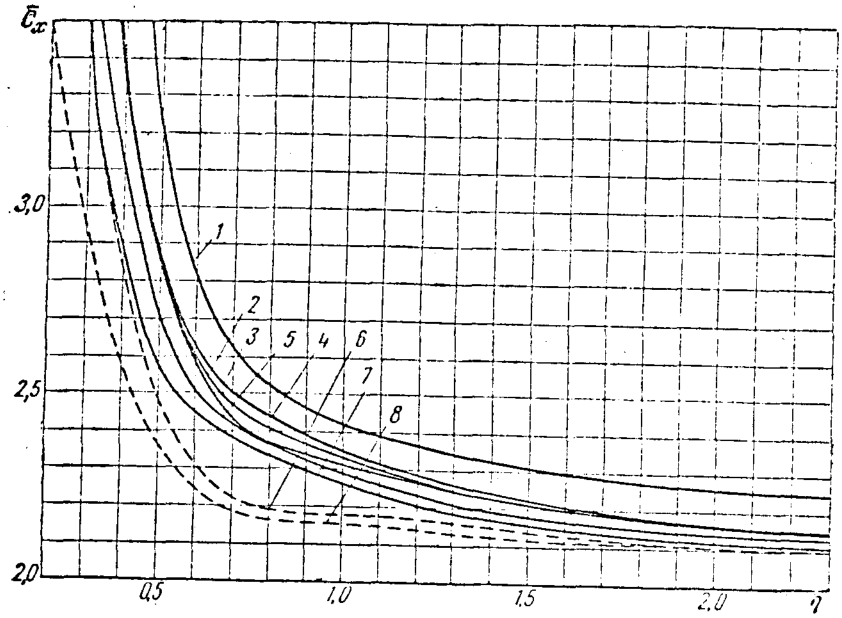

Figure 9. Drag Coefficient of Blunted Cone in Similarity Variables (symbols as on Figure 7)

Physical and chemical processes influence strongly the flow of the gas around a blunted body. First of all, as was noted earlier in [4], the area of influence of blunting is reduced significantly. A similar conclusion was produced theoretically [19] in an analysis of flows with various ratios of heat capacities γ. In connection with this, in the area of this influence, parameters P, ζ and $\bar{C}_x$ calculated with and without consideration of physical-chemical reactions differ strongly from each other, as we can see on Figures 7-12. In particular, with equilibrium flow the drag coefficient of a blunted cone may exceed the drag coefficient of this same cone penetrating an ideal gas with γ = 1.4 by 10% or more (Figures 9 and 12). Comparison of curves 2, 3 and 4 on Figures 7-9 and 10-12 shows that the influence of pressure and temperature in the oncoming stream is not too great within the range of change of these parameters which we analyzed, and can be easily considered using various types of correcting coefficients. /223

The solutions from the theory of hypersonic flows [19] indicated the presence of a drag minimum for a blunted cone. According to the theory, the relative decrease in the drag coefficient may reach 10% in comparison with a corresponding sharp cone.

The results of calculations shown on Figures 9 and 12 confirm this conclusion of the theory qualitatively: with hypersonic flow around a blunted cone, the drag coefficient actually does have a minimum -- see curves 5, 7 and 8 on Figure 12.

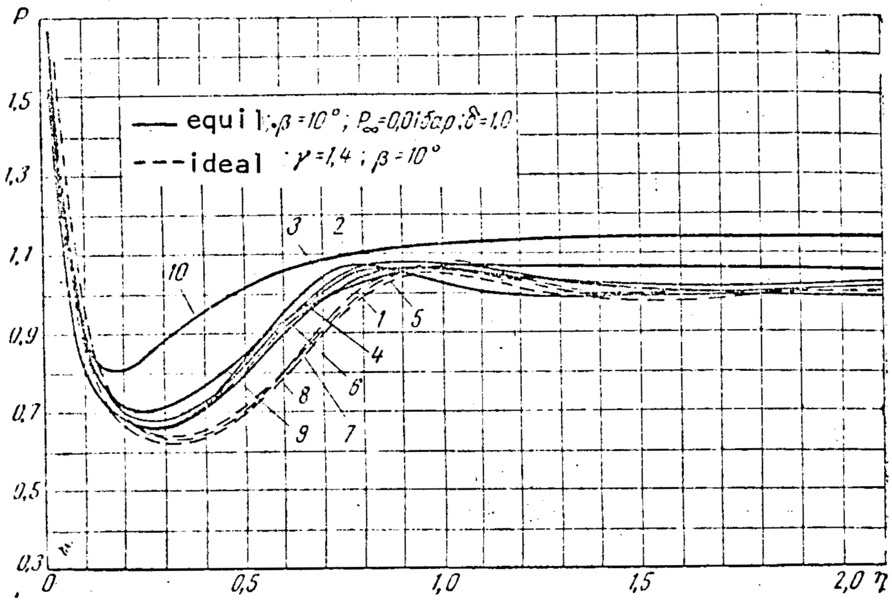

Figure 10. Pressure on Surface of Blunted Cone in Similarity Variables in Case of Flow of Ideal and Equilibrium Gas (Air)

M_∞	C_{x_0}	T_∞ [° K]	M_∞	C_{x_0}	δ
1—25	0,924	250	5—20	0,905	1
2—20	0,926	200	7—∞	0,420	1/3
3—20	0,926	300	8—∞	0,569	0,5
4—20	0,926	250			
6—15	0,917	250			
9—10	0,933	250			
10—6	0,902	250			

As the blunting is increased (corresponding to an increase in C_{x0}) and angle β is decreased (curves 6 and 8 on Figure 9 and curves 5, 7 and 8 on Figure 12) this singularity appears more clearly; the minimum appears at $\beta \lesssim 10°$.

Consideration of equilibrium physical-chemical reactions results in a sharp decrease in the area of influence of the blunting, and the drag minimum is not observed.

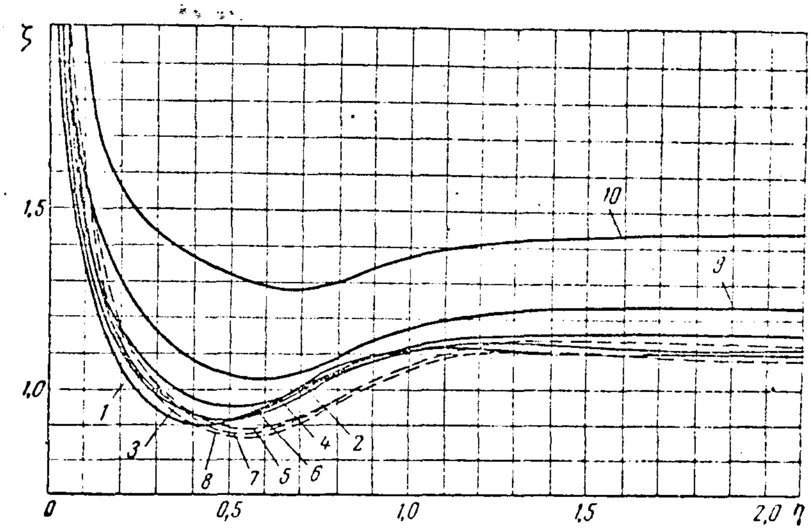

Figure 11. Inclination of Head Wave to Direction of Oncoming Stream in Similarity Variables for Flow Around Blunted Cone (symbols as on Figure 9)

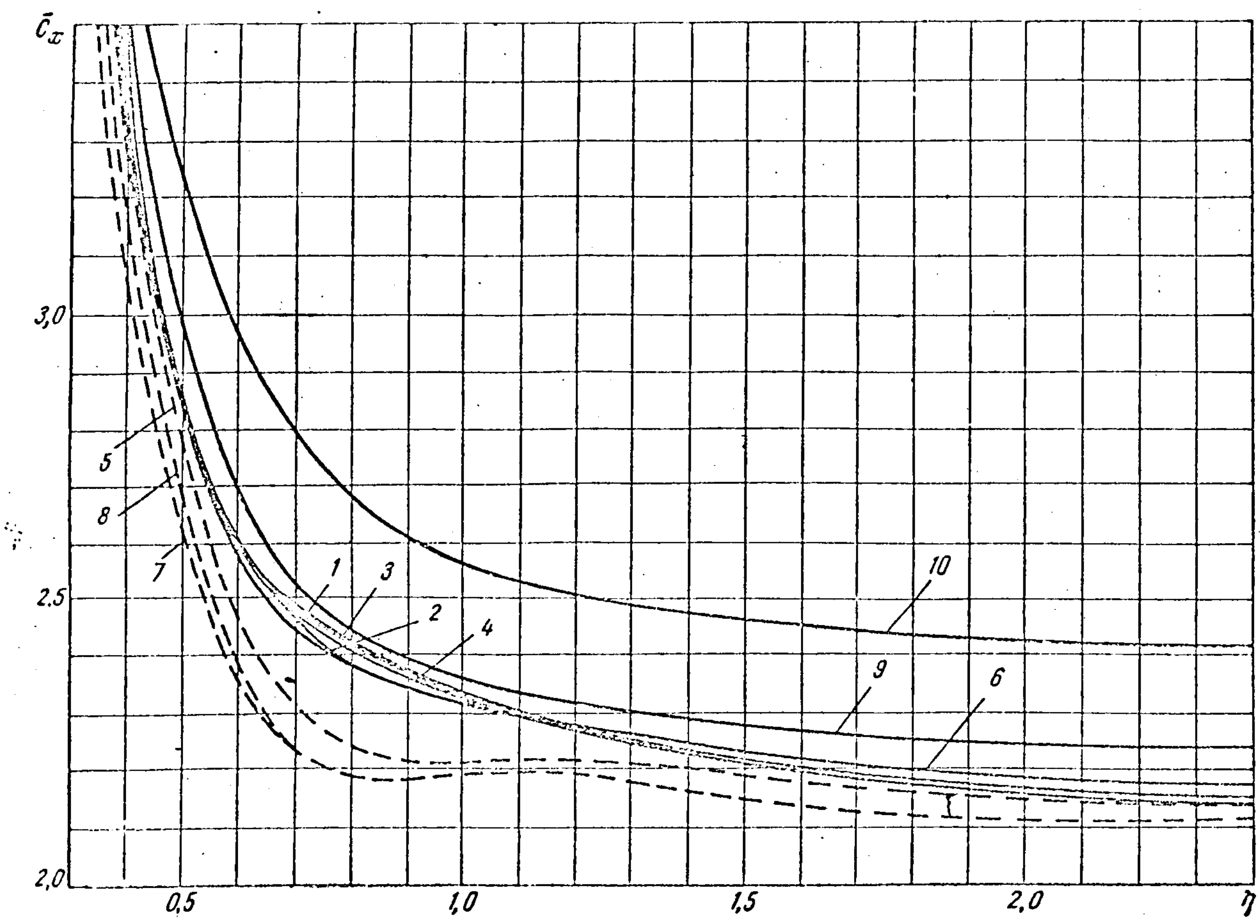

Figure 12. Drag Coefficient of Blunted Cone in Similarity Variables (symbols as on Figure 9)

REFERENCES

1. Babenko, K. I., G. P. Voskresenskiy, "A Numerical Method for Calculating Three-Dimensional Flow of a Supersonic Gas Stream Around Bodies," *Zhurnal Bychislitel'noy Matematiki i Matem. Fiz.*, Vol. 1, No. 6, 1961.
2. Babenko, K. I., G. P. Voskresenskiy, A. N. Lyubimov, V. V. Rusanov, *Prostranstvennoye Obtekaniye Gladkikh Tel Ideal'nym Gazom* [Three-Dimensional Flow of an Ideal Gas Around Smooth Bodies], Nauka Press, Moscow, 1964.
3. D'yakonov, Yu. N., N. A. Zaytseva, "Supersonic Flow of an Ideal Gas Around a Blunted Body," *Izvestiya Akademii Nauk SSSR, Seriya Mekhaniki i Mashinostroyeniya*, No. 1, 1963.
4. D'yakonov, Yu. N., "Three-Dimensional Flow Around Blunted Bodies in Consideration of Equilibrium Physical-Chemical Reactions," *Doklady Akademii Nauk SSSR*, Vol. 157, No. 4, 1964.
5. D'yakonov, Yu. N., "Three-Dimensional Supersonic Flow of an Ideal Gas Around Blunted Bodies," *Izvestiya Akademii Nauk SSSR, Seriya Mekhaniki i Mashinostroyeniya*, No. 4, 1964.
6. Chushkin, P. I., "Simple Form Blunted Bodies in Supersonic Gas Flow," *Prikladnaya Matematika i Mekhanika*, Vol. 24, No. 5, 1960.
7. Roslyakov, G. S., N. V. Drozdova, "Numerical Calculation of Flow Around a Stepped Cone," *Chislennyye Metody v Gazovoy Dinamike* [Numerical Methods in Gas Dynamics], No. 2, Moscow State University Press, 1963.
8. Moretti, G., "Three-Dimensional Supersonic Flow Computations," *AIAA Journal*, Vol. 1, No. 9, 1963.
9. Zapryanov, Z. D., V. B. Minostsev, "Method for Calculation of Three-Dimensional Supersonic Flow Around Bodies," *Izvestiya Akademii Nauk SSSR, Seriya Mekhaniki i Mashinostroyeniya*, No. 5, 1964.
10. Rusanov, V. V., "Characteristics of General Gas Dynamics Equations," *Zhurnal Bychisl. Matem. i Matem. Fiz.*, Vol. 3, No. 3, 1963.
11. Katskova, O. N., P. I. Chushkin, "Three-Dimensional Supersonic Equilibrium Gas Flow Around Bodies Under Angle of Attack," *Zhurn. Vychisl. Matem. i Matem. Fiz.*, Vol. 5, No. 3, 1965.
12. Ehlers, F. E., "The Method of Characteristics for Isoenergetic Supersonic Flows Adapted to High Speed Digital Computers," *Xoc. Industr. and Appl. Math.*, Vol. 7, No. 1, 1959.
13. Predvoditelev, A. S., Ye. V. Stupochenko, et al., *Tablitsy Termodinamicheskikh Funktsii Vozdukha* [Tables of Thermodynamic Functions for Air], Computer Center, Academy of Sciences USSR, 1962. /224
14. Predvoditelev, A. S., Ye. V. Stupochenko, et al., *Tablitsy Termodinamicheskikh Funktsiy Vozdukha* [Tables of Thermodynamic Functions for Air], Academy of Sciences USSR Press, Moscow, 1957.
15. Predvoditelev, A. S., Ye. V. Stupochenko, et al., *Tablitsy Termodinamicheskikh Funktsiy Vozdukha* [Tables of Thermodynamic Functions for Air], Academy of Sciences USSR Press, Moscow, 1959.
16. Gilinskiy, S. M., G. F. Telenin, G. P. Tinyakov, "Method of Calculating Supersonic Flow Around Blunt Bodies with Receding Shock Wave," *Izvestiya Akademii Nauk SSSR, Seriya Mekhaniki i Mashinostroyeniya*, No. 4, 1964.

17. Telenin, G. F., G. P. Tinyakov, "Method of Calculating Three-Dimensional Flow Around Bodies with Receding Shock Wave," *Doklady Akademii Nauk SSSR*, Vol. 154, No. 5, 1964.
18. Telenin, G. F., G. P. Tinyakov, "Investigation of Supersonic Flow Around a Sphere by Air and Carbon Dioxide at Thermochemical Equilibrium," *Doklady Akademii Nauk SSSR*, Vol. 159, No. 1, 1964.
19. Chernyy, G. G., *Techeniye Gaza s Bol'shoy Sverkhzvukovoy Skorost'yu* [Gas Flow at High Supersonic Velocity], Fizmatgiz. Press, Moscow, 1959.

Translated for the National Aeronautics and Space Administration under contract No. NASw-1695 by Techtran Corporation, P. O. Box 729, Glen Burnie, Maryland 21061